First dehydrogenation of ethanol catalyzed by a single atom of d-block metals

Kaitlyn R. Wiegand, Ruitao Wu, Peshala K. Jayamaha, Delaney Collazo, and Lichang Wang*
School of Chemical and Biomolecular Sciences and the Materials Technology Center,
Southern Illinois University, Carbondale, Illinois 62901, USA

ABSTRACT

The initial dehydrogenation of ethanol is important in the development of sustainable and practical energy processes. Transition metals, especially the less expensive and more abundant 3d metals, are appealing as catalysts for ethanol dehydrogenation. As a single atom adsorbed to ethanol, these metals are likely to have enhanced selectivity and activity, in addition to maximized utilization efficiency. Density functional theory calculations were performed with Gaussian16 to investigate these ideas using both the B3PW91 and PBEPBE functional. The presented work explores the use of 18 different single metal atoms as catalysts in the first dehydrogenation of ethanol. All of the 3d metals, as well as eight 4d and 5d metals, were investigated as catalysts for this reaction. Three ethanol dehydrogenation pathways were studied for each metal catalyst: α-H, β-H, and *o*-H cleavage. Analysis of the energies of each reaction allowed for a determination of the dehydrogenation pathway most favored by each metal catalyst, and ultimately yielded a top catalyst for each dehydrogenation pathway. Based on the results of these calculations, the best predicted catalyst for *o*-H cleavage was scandium, for β-H and α-H cleavage was platinum. However, differences in the B3PW91 and PBEPBE results suggest that β-H cleavage could also be favored for Pt, and that another possible top catalyst for β-H cleavage could be Pd. This work will serve as a benchmark for heterogeneous catalysis of the ethanol dehydrogenation reaction.

* Correspondence author: lwang@chem.siu.edu (E-mail).

1. Introduction

An increasingly relevant ambition in current research is the desire to develop methods for producing sustainable, environmentally friendly energy that is both economically and realistically feasible for fulfilling our world's energy needs.[1] According to a 2020 IEA world energy outlook report, if the infrastructure currently in place and the power plants currently under construction were to be operated at similar levels as they are today, using natural gas combustion as the primary source of energy, our world would see a 1.65°C increase in temperature with 10 Gt of continued CO_2 emission from these sources in 2050.[2] The projected energy needs going forward into 2040 come with an increase in high quantities of oil and natural gas as the primary sources with continued use of coal, all of which are nonrenewable.[3]

Biofuels are an appealing source of alternative energy, as they are made from biomass and are therefore renewable.[4] Ethanol, a well-known biofuel, is added in various percentages to about 97% of the gasoline used in the U.S., which decreases the amount of crude oil used to produce petroleum fuels.[4,5] This, plus the fact that ethanol burns cleaner than the pure fuels, helps lower emissions of pollutants like carbon monoxide.[4,5] Due to it already being established as a widely-used biofuel, further utilization of ethanol as a renewable energy source in other sustainable-energy processes is attractive.

There are three types of hydrogens in an ethanol molecule: the hydrogen that bonds to O atom, denoted as *o*-H; two hydrogen that bond to the α-C, i.e. α-H; three hydrogen that bond to the β-C, i.e. β-H. Therefore, there are theoretically three reaction pathways in the first dehydrogenation of ethanol. Ethanol dehydrogenation to produce hydrogen gas, a clean and efficient energy source, has made this reaction very promising as a source of energy that is sustainable, renewable, and low-cost.[1] Ethanol steam reforming (ESR) is a very efficient process that produces hydrogen via

the dehydrogenation of ethanol.[6] The overall reaction of ESR is: C_2H_5OH (g) + $3H_2O$ (g) → $2CO_2$(g) + $6H_2$(g), where the first step is the selective dehydrogenation of ethanol at the oxygen and alpha carbon.[6] It has been found for ESR that decreasing the size of metal catalysts brings an increase in the activity and stability of the catalyst.[6] While highly active catalyst systems involving noble metals like rhodium, ruthenium, platinum, and palladium have been found to catalyze ESR, the expensive nature of these metals makes them an unreasonable option for large-scale production of hydrogen for energy.[6]

Ethanol dehydrogenation reaction is industrially very important, not only to produce hydrogen for clean energy technology but also as starting materials to synthesize value-added molecules for many other applications,[7-25] and it can be efficiently enhanced by the SACs. Ethanol dehydrogenation can take place via many reaction pathways and produce different products. Catalytic dehydrogenation via O-H and C-H bond cleavage can produce acetaldehyde and H_2.[1] C-C and C-O bond scission steps occur in deoxygenation, decomposition, and reforming reactions and will end up with many different products along with H_2 and other byproducts.[1,26] Non-oxidative ethanol dehydrogenation is one of the most potential routes for acetaldehyde and H_2 production.[27] Produced H_2 through a non-oxidative pathway is clean and doesn't require a separation process.[28] So, it is important to develop stable and selective catalysts for ethanol dehydrogenation reactions.

Besides using ethanol dehydrogenation for hydrogen production, ethanol can also be utilized directly in direct ethanol fuel cells (DEFCs) to generate energy.[29-32] The utilization of DEFCs could be an optimal solution since the storage and transportation of H_2 is not well established, and the process is CO_2 neutral.[33] In DEFCs, the complete oxidation of ethanol, $C_2H_5OH + 3O_2 \rightarrow 2CO_2 + 3H_2O$, can be carried out to produce twelve electrons.[33] Despite the incredible potential for DEFCs

to be used as an efficient and environmentally friendly source of high density energy, the high energy barrier of C-C bond cleavage[34-36] can limit their prospective use as large-scale energy sources.[29] Therefore, a lot of research efforts have been devoted to understand catalytic EOR.[31,37-61] From our previous work, we found that the activation barrier of ethanol C-C bond cleavage on an Ir(100) surface was always lowered with the removal of the hydrogen from oxygen.[62] Thus, selective ethanol dehydrogenation could potentially be utilized to lower this C-C bond cleavage in order to make the complete oxidation of ethanol a more favorable process, thereby making DEFCs a more viable option in the world of sustainable energy.

Copper-based catalysts were considered a highly selective and reactive metal for ethanol dehydrogenation reactions[63-66] but suffered from the low activity and particle sintering.[67] Gold-based catalysts also showed promising catalytic activity toward ethanol dehydrogenation with higher sintering resistance.[68] A silica-supported Ag catalyst has been shown to be an efficient heterogeneous catalyst for non-oxidative ethanol dehydrogenation into acetaldehyde and H_2.[69] A series of alloys containing Pd-Ru, Pd-Ag, Pd-Rh, and Pd-Ni has been shown higher catalytic activity for ethanol dehydrogenation and excellent hydrogen formation capability.[1] Georgios reported that NiAu single-atom alloy shows promising catalytic properties for nonoxidative ethanol dehydrogenation.[70] Most of the d-block metals are used in the ethanol dehydrogenation experiments as the catalyst.

Catalytic oxidation and dehydrogenation reactions have been successfully achieved with single-atom catalysts (SACs) in recent years.[71] Single-atom catalysts (SACs) have been shown experimentally and theoretically to catalyze a number of reactions with high activity,[40,72-94] may also be used to catalyze ethanol dehydrogenation.[95] In single atom catalysis, isolated metal atoms, which are generally stabilized by the support of or by alloying with another metal, are the only

active metal catalyst.[95,96] While free single atoms possess a high surface energy, rendering them unstable on their own, strong interaction with a metal support lowers the single atom's surface energy to help prevent aggregation.[95,96] Since the catalyst is a single atom, the utilization efficiency of the metal being used is at a maximum, and the cost of the catalyst is reduced relative to other catalysts involving the same metal.[95-97] The small size of SACs, as well as their ability to be uniformly distributed on surfaces, gives them an increased catalytic selectivity and activity.[95,96] This is so much so, that they have been found to be hundreds of times more active per atom than nanoparticle catalysts.[95] When looking for a metal species to act as a SAC in ethanol dehydrogenation, it is important to note that transition metals have generally been found to catalyze the removal of hydrogen from saturated molecules with high efficiency and selectivity.[71] SACs made of 3d transition metals are of interest because of their potential to be more sustainable due to their abundance, durability, and decreased toxicity relative to other 4d and 5d metals.[98,99] However, the variability in electronic structure, oxidation state, and atomic radii of transition metals has an impact on their catalytic ability, making it necessary to determine how these different metals may catalyze various reactions.[71]

The need for a sustainable and practical energy source may be one step closer to being met if an efficient catalyst for ethanol dehydrogenation can be found, so that the dehydrogenated products can be utilized in further reactions to produce energy. In searching for this catalyst, we systematically studied all three types of ethanol dehydrogenation reactions in the presence of a single metal atom of the ten third row metals, as well as eight other metals: Ru, Rh, Pd, Ag, Os, Ir, Pt, and Au, using DFT calculations. B3PW91 is often used in the studies of ethanol dehydrogenation on metal clusters[99], but PBE is often the choice of functional in the studies of catalysis on bulk materials. To allow better comparisons with single atom, cluster, or bulk models,

we chose to perform calculations using both B3PW91 and PBE. We note that single atom catalysis has become a hot topic recently due to advanced characterization becoming available.[100]

These calculations were performed with the intention of identifying the dehydrogenation pathway of ethanol as a function of the metal catalyst used. Further, they were completed in order to determine which metal(s) is/are the best for the selective dehydrogenation of *o*-H, α-H, or β-H. Computations were performed using two different functionals to see how the choice of functional affected the preferred pathway of dehydrogenation for each metal catalyst, and if the overall top catalysts for each type of ethanol dehydrogenation was consistent between the models.

2. Computational Details

The results presented are those of DFT computations performed using Gaussian16. Eighteen metals were studied as catalysts for the dehydrogenation of ethanol, including all of the row 3d metals (Sc, Ti, V, Cr, Mn, Fe, Co, Ni, Cu, Zn), four 4d metals (Ru, Rh, Pd, Ag), and four 5d metals (Os, Ir, Pt, Au). For each metal, computations were performed for the cleavage of the α-H, β-H, and *o*-H of ethanol. The initial state (IS) of each dehydrogenation was characterized by a single metal atom bonded to the oxygen of ethanol, and each final state (FS) molecule was such that the metal atom was inserted between the atoms of the bond being cleaved.

Calculations were performed using both the B3PW91 functional and the PBEPBE functional, so the results of each could be compared. The spin multiplicities used for each metal, based on the relative stability of the IS structure at that spin, are given in Table 1. For calculations performed using the B3PW91 functional, the 6-311G(d,p) basis set was used for C, H, and O atoms. For calculations completed with the PBEPBE functional, the 6-311++G(d,p) basis set was used for C, H, and O atoms. For all calculations, the LANL2DZ basis set was used for the single metal atom.

To ensure the IS and FS structures were optimized to a minimum, frequency calculations were performed so the structure could be checked to have no imaginary vibrational frequencies. Transition state (TS) structures were found using TS (Berny), QST2, and QST3 methods. Intrinsic reaction coordinate calculations (IRC) were completed to verify that the TS structure led to the FS structure. All TS structures were made sure to have only one imaginary vibrational frequency.

For those reactions which transition states were not found, we used the relationship between reaction energy (ΔE) and activation energy (E_a) of ethanol dehydrogenation reaction using the Bronsted-Evans-Polanyi (BEP) correlation method to predict the activation barriers. Many of the computational studies associated with the difficulties in finding and characterization the transition structures have been overcome those difficulties with the using the Bronsted-Evans-Polanyi (BEP) relationship, by linearly relating the activation barrier to the reaction energy or adsorption energy.[101 102]

Table 1: Spin multiplicities of predicted ground electronic state of metal atom.

Metal	Spin Multiplicity
Sc	2
Ti	3
V	6
Cr	7
Mn	6
Fe	5
Co	4
Ni	3
Cu	2
Zn	1
Ru	5
Rh	2
Pd	1
Ag	2
Os	5
Ir	4
Pt	1
Au	2

For each metal catalyst tested, adsorption energy of the metal on ethanol (E_{ads}) was calculated. This, as well as the reaction energy (ΔE) and activation energy (E_a) of each dehydrogenation reaction were calculated using the equations:

$$E_{ads} = E_{IS} - E_{CH_3CH_2OH} - E_M \quad (1)$$

$$\Delta E = E_{FS} - E_{IS} \quad (2)$$

$$E_a = E_{TS} - E_{IS} \quad (3)$$

where E_{IS}, E_{FS}, and E_{TS} are the total energies of the IS, FS, and TS, respectively, that have been corrected for zero-point energy (ZPE). $E_{CH3CH2OH}$ and E_M are the ZPE-corrected energies of ethanol and the single metal atom, respectively. All energies presented here have been corrected for ZPE using:

$$E_{ZPE} = \sum_{i=1}^{k} \frac{h\nu_i}{2} \quad (4)$$

where all non-imaginary vibrational frequencies (ν_i) are summed together after being multiplied by the Planck's constant (h) and divided by two.

3. Results and Discussion

3.1 Adsorption of ethanol to metals

For the following results shown in Figure 1, numerical values are assigned to metals for the purpose of plotting data as a function of metal. The 18 metals studied, and their corresponding numerical identities are given in Table 2.

Table 2: Numerical values assigned to metals in Figure 1.

	3d Metal	4d Metal	5d Metal
1	Sc		
2	Ti		
3	V		
4	Cr		
5	Mn		
6	Fe	Ru	Os
7	Co	Rh	Ir
8	Ni	Pd	Pt
9	Cu	Ag	Au
10	Zn		

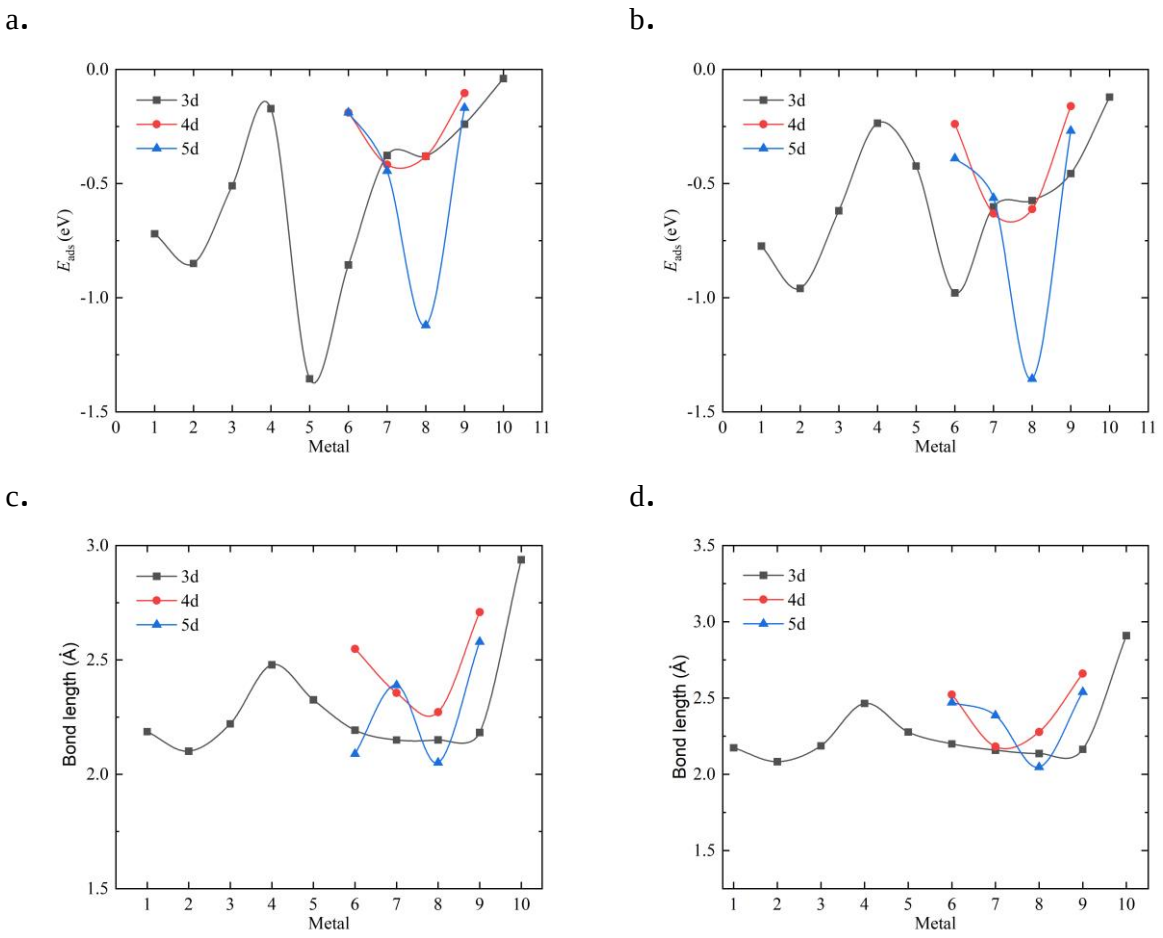

Figure 1: Adsorption energies of metals onto the oxygen of ethanol, calculated using the B3PW91 functional (a) and the PBEPBE functional (b). O-M bond length for metals, calculated using the B3PW91 functional (c) and the PBEPBE functional (d).

Obtaining the adsorption energy of a single metal atom onto the oxygen of ethanol is the first step in determining whether or not the upcoming dehydrogenation reaction could be feasible. A positive adsorption energy indicates that the formation of the initial state, and therefore the continuation of the ethanol dehydrogenation reaction, is thermodynamically nonspontaneous. A negative energy translates to a thermodynamically favorable process, which will allow further reaction of the initial state species. Adsorption energies are plotted as a function of metal in Figure 1, based on calculations performed using the B3PW91 and PBEPBE functional. For both sets of data, the adsorption energies of all 18 metals onto ethanol are negative, meaning any of the metals could theoretically go on to catalyze the dehydrogenation of ethanol. There is some difference between the two functionals, with most differences ranging between 0.2 and 0.05 eV, and the largest being that of Mn, 0.93 eV.

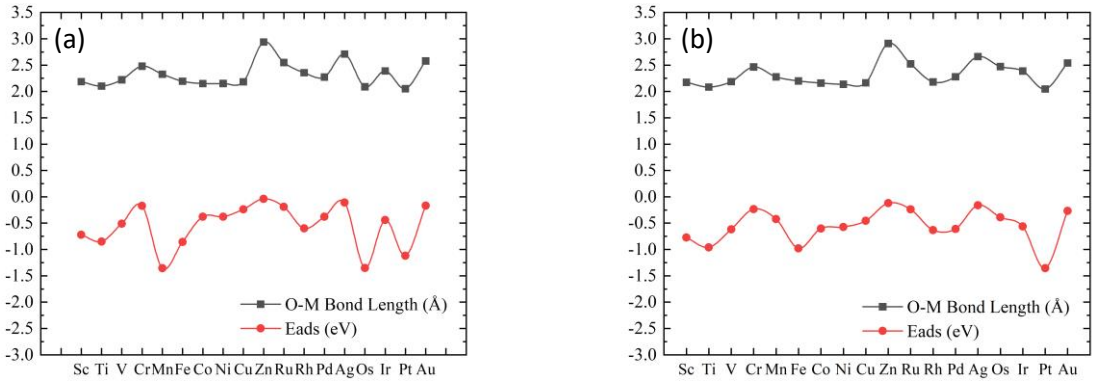

Figure 2: Plots of O-M bond length and adsorption energy for metals, calculated using the B3PW91 functional (a) and the PBEPBE functional (b).

An interesting comparison to make is with the oxygen-metal (O-M) bond length of the IS species and the adsorption energy of the metal onto the oxygen (Fig. 2). Visually, by looking at the plots of O-M bond length and Eads, there appears to be a relation between the two. For most

metals, the more favorable the adsorption, indicated by a more negative energy, the shorter the O-M bond. This is the case for both the B3PW91 and the PBEPBE functional.

3.2 Ethanol dehydrogenation: α-H, β-H, and *o*-H

The DFT results of dehydrogenation in the presence of a single metal atom are presented and compared first based on the row that the metal atoms are and then the group.

3.2.1 3d metal-catalyzed dehydrogenation

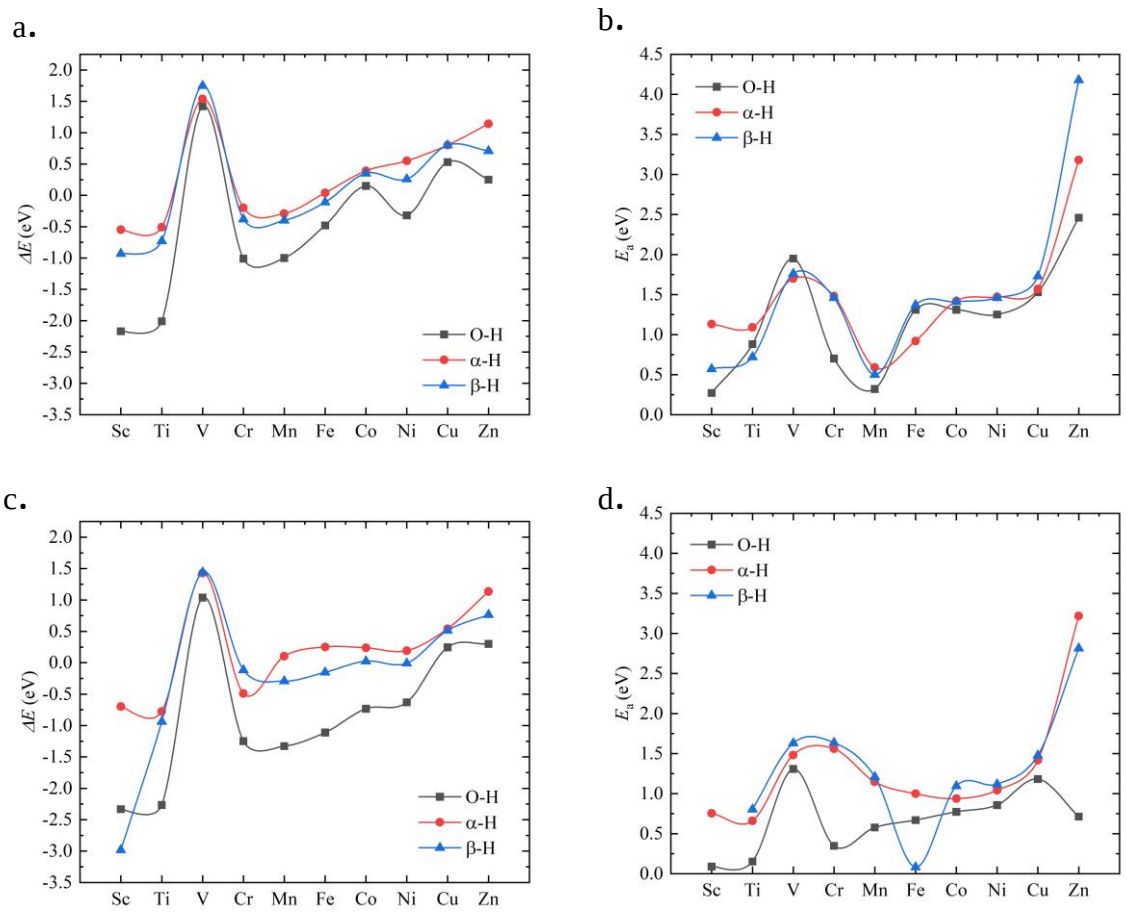

Figure 3: Activation energies and reaction energies of α-H, β-H, and *o*-H dehydrogenation catalyzed by 3d metals, including a) ΔE calculated using the B3PW91 functional, b) Ea calculated using the B3PW91 functional, c) ΔE calculated using the PBEPBE functional, and d) Ea calculated using the PBEPBE functional.

The overall trend in reaction energy of 3d metal-catalyzed dehydrogenation is to increase from left to right across the period (Fig. 3). There are, however, large jumps in reaction energy for dehydrogenation reactions catalyzed by V, which disrupt this trend. These observations are true for both functionals, at all three locations of ethanol dehydrogenation. For most metals, the reaction energies of *o*-H dehydrogenation are the lowest, and those of α-H dehydrogenation are the greatest. Exceptions to this are V, for which the β-H dehydrogenation reaction energy is the greatest for both functionals, and for Sc when modeled by the PBEPBE functional, which has a very negative reaction energy for β-H dehydrogenation. It should be noted that these results can change slightly, depending on which β-H is removed. If the metal is positioned trans to the oxygen of ethanol on the β-C, the reaction energies of β-H are mostly greater than those of α-H. If the metal is positioned cis to the oxygen of ethanol on the β-C, as was done to obtain these results, the reaction energies of β-H are mostly lower than those of α-H.

For most reactions, the reaction energies calculated using the PBEPBE functional are more negative than those calculated using the B3PW91 functional. The difference in reaction energy between the two functionals is fairly small (0.1 to 0.4 eV) for most all metals at three dehydrogenation locations. However, there is a large difference of 2.05 eV in the ΔE of Sc-catalyzed β-H removal. As previously noted, this reaction energy, when calculated using the PBEPBE functional, is very negative. One would not expect this to be the case based on the results obtained using the B3PW91 functional, and on the trend in reaction energy for Sc-catalyzed α-H and *o*-H dehydrogenation. Thus, it could be that this unusually negative reaction energy is a result of error in the structure of the FS following β-H cleavage by Sc.

Relative to the plots of reaction energies, the plots of the activation energies are much less cohesive. For Sc, TS structures were not able to be found for β-H and o-H dehydrogenation

reactions. So, activation barriers were predicted using the Bronsted-Evans-Polanyi (BEP) relationship. Despite these things, it remains that for most reactions, the activation barriers are lowest for *o*-H dehydrogenation. As for α-H and β-H dehydrogenation modeled with the PBEPBE functional, there is variability between the metals as to which kind of dehydrogenation is more favorable. This variability lessens with the use of the B3PW91 functional, which shows most barriers being greater for β-H dehydrogenation.

Using the criteria that for a reaction to proceed favorably under room temperature, it must have an exothermic reaction energy and an activation barrier of less than around 0.72 eV, the results of both functionals reveal that of the 3d metals, V and Cu would not catalyze any of the dehydrogenation pathways of ethanol. These metals have both positive reaction energies and high activation barriers. Other metals, which have exothermic reaction energies for some dehydrogenation pathways, but have high activation barriers for all three pathways, include Cr. Thus, Cr would not be good catalysts. Of the remaining 3d metals that have favorable reaction and activation energies for at least one of the dehydrogenation pathways (Sc, Ti, Mn, Fe), *o*-H dehydrogenation has the lowest reaction energy and activation barrier when catalyzed by Sc.

As for α-H dehydrogenation, Ti is the only 3d metal with a negative ΔE and small E_a (0.66 eV), but only when the reaction was modeled with the PBEPBE functional. When calculated using the B3PW91 functional, the activation barrier is larger (1.09 eV). While Fe does have favorable energies for β-H dehydrogenation when calculated using the PBEPBE functional, there are significant differences in these energies when calculated using the B3PW91 functional. The results of the B3PW91 functional point towards Fe being an unfavorable catalyst for β-H dehydrogenation. The reaction energies of Sc-catalyzed β-H dehydrogenation for both functionals are negative, but the E_a could not be obtained with the PBEPBE functional, leaving only the

B3PW91 result to analyze. Due to these discrepancies, it cannot be determined whether any of the 3d metals could favorably catalyze β-H dehydrogenation of ethanol.

3.2.2 4d metal-catalyzed dehydrogenation

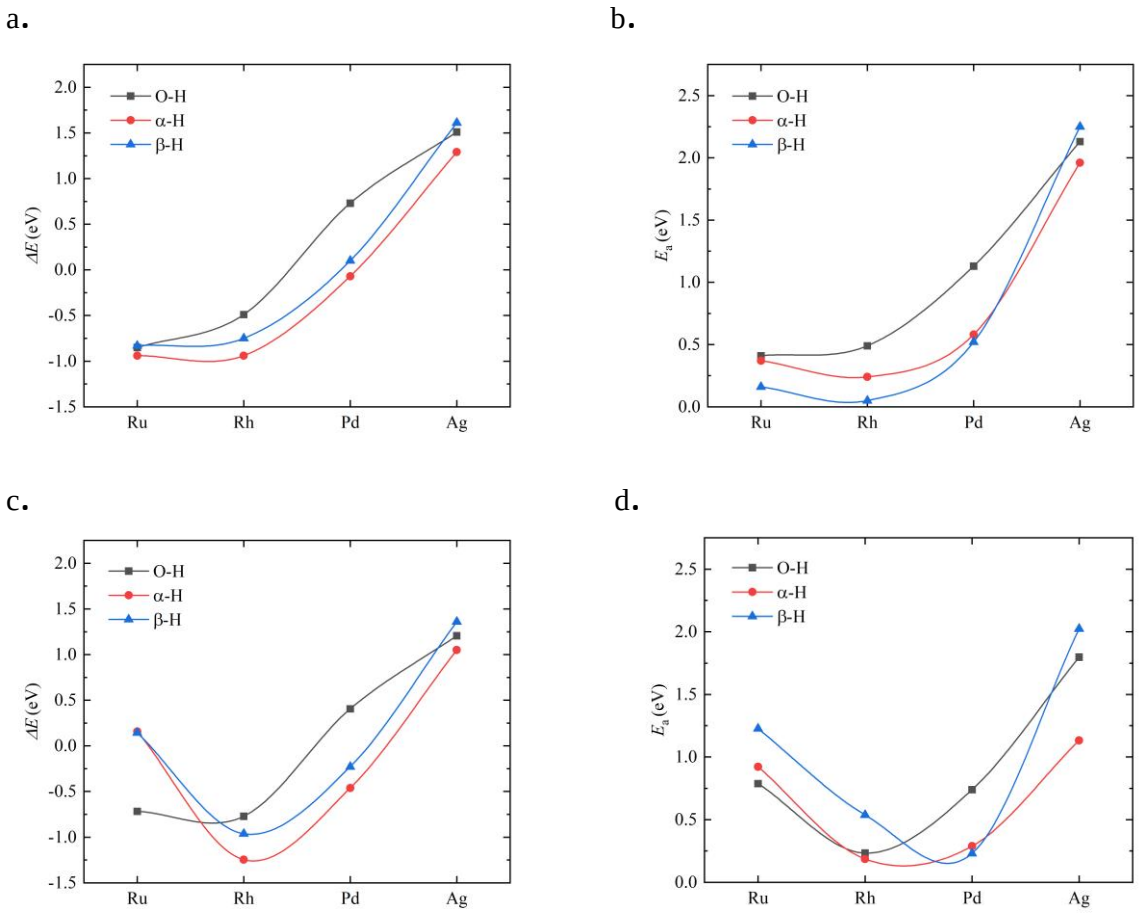

Figure 4: Activation energies and reaction energies of α-H, β-H, and *o*-H dehydrogenation catalyzed by 4d metals, including a) ΔE calculated using the B3PW91 functional, b) Ea calculated using the B3PW91 functional, c) ΔE calculated using the PBEPBE functional, and d) Ea calculated using the PBEPBE functional.

The trends in reaction energy of ethanol dehydrogenation when catalyzed by 4d metals except Ru, are very similar between the B3PW91 and PBEPBE functionals (Fig. 4). The shapes of the plots are almost identical, with the difference being that the energies calculated with the

PBEPBE functional are all around 0.3 eV lower than those calculated using the B3PW91 functional. According to the results of both functionals, α-H dehydrogenation is most thermodynamically favorable when catalyzed by Rh and Pd, but *o*-H dehydrogenation is more favorable when catalyzed by Ru. The trends in activation energies also appear to be similar between the two functionals. Once again, the energies calculated using the PBEPBE functional are all 0.2-0.4 eV less than those calculated using the B3PW91 functional, with some differences being larger, such as the 0.83 eV difference for Ag-catalyzed α-H dehydrogenation. Activation energy barrier for β-H dehydrogenation using Rh and Ru were obtained using BEP relation for further analysis of the study. It seems β-H dehydrogenation is more kinetically favorable with Rh and Pd as catalysts.

Of the 4d metals, Ag is the only one that has both high activation energies (> 1 eV) and positive reaction energies for all three dehydrogenation pathways, making it a poor catalyst for ethanol dehydrogenation. This is true for both functionals. All three dehydrogenation reactions have the most negative reaction energies and low activation barriers with Rh as a catalyst. The B3PW91and PBEPBE results for this set of data reveal a very low activation barrier (0.05 eV), so Rh is accepted as the best catalyst of the 4d metals when paired with the fact that is also has the most negative reaction energy. The ΔE of α-H dehydrogenation via Rh is more negative than β-H dehydrogenation whe using the PBEPBE functional, but the activation barrier of α-H dehydrogenation is lower, predicting α-H dehydrogenation to occur first. Pd could also potentially act as a good catalyst in the α-H and β-H dehydrogenation of ethanol, but it does not have as favorable energies as Rh. Differences between the two functionals make it difficult to discern which reaction pathway Pd would prefer to catalyze. The activation barriers of β-H dehydrogenation for both functionals are lower than α-H dehydrogenation, but the reaction energy

of β-H dehydrogenation calculated using B3PW91 is positive, whereas it is negative using PBEPBE. The reaction energies of Pd-catalyzed α-H dehydrogenation are more exothermic than β-H for both functionals. However, Pd is a better dehydrogenation catalyst[103,104] than other metals, such as Rh based on the comparison of overall reaction energy.

3.2.3 5d metal-catalyzed dehydrogenation

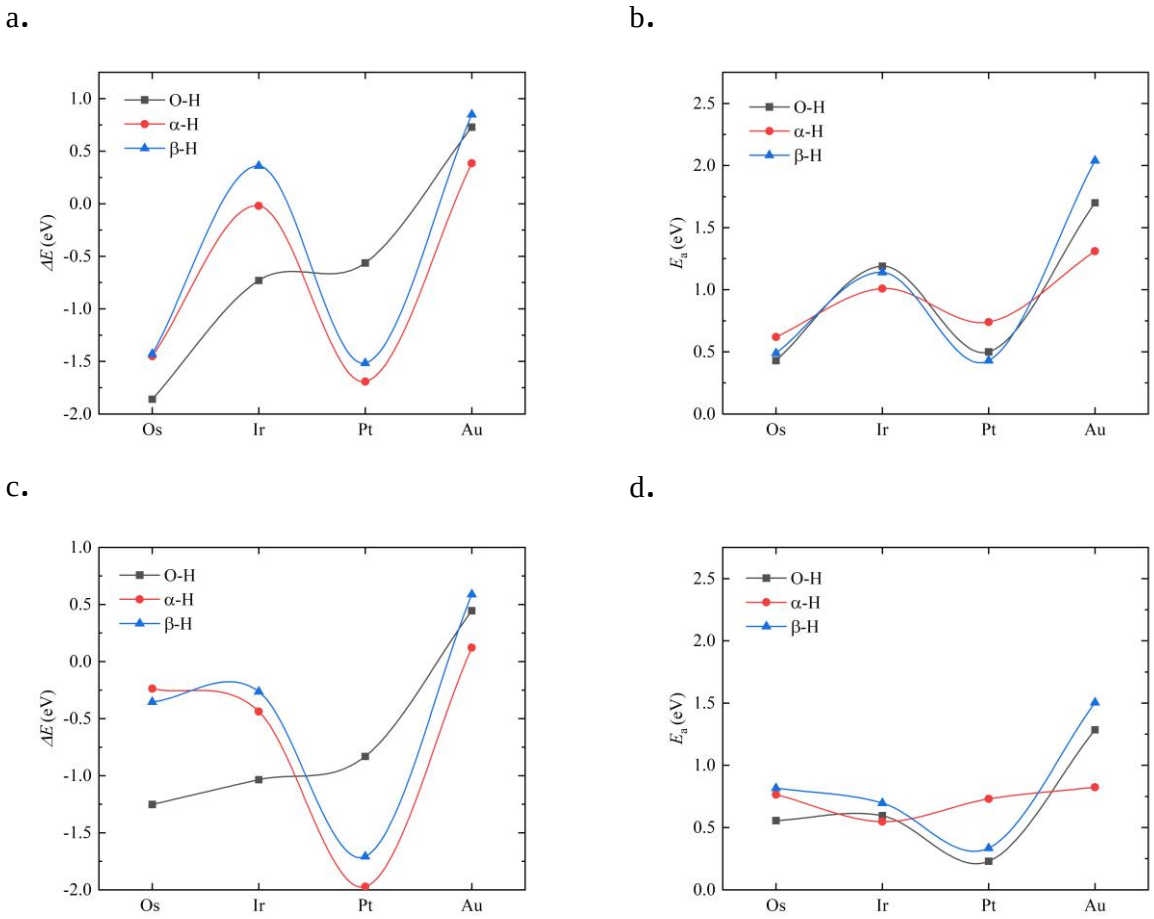

Figure 5: Activation energies and reaction energies of α-H, β-H, and *o*-H dehydrogenation catalyzed by 3d metals, including a) ΔE calculated using the B3PW91 functional, b) Ea calculated using the B3PW91 functional, c) ΔE calculated using the PBEPBE functional, and d) Ea calculated using the PBEPBE functional.

Once again, there is a large similarity between the plots of reaction energy for the B3PW91 and PBEPBE functional for 5d metal-catalyzed dehydrogenation (Fig. 5). The PBEPBE energies are lower than B3PW91, many by 0.1-0.3 eV, and some by lesser amounts, as small as 0.02 eV. Most activation barriers obtained for the two functionals have a difference of around 0.3-0.5 eV, with some being as small as 0.006 eV.

The energies of Au-catalyzed dehydrogenation are thermodynamically and kinetically unfavorable for every pathway, making it a poor catalyst for this purpose. This is true for the results of both functionals. According to the B3PW91 results, Ir would be an unlikely catalyst due to the high activation barriers of every dehydrogenation reaction, despite having exothermic reaction energies for α-H and *o*-H dehydrogenation. However, all of these reactions have lower activation barriers (≤0.72 eV) and negative reaction energies when calculated using the PBEPBE functional. Thus, results for Ir are inconclusive. Between Os and Pt, they could both catalyze α-H, β-H and *o*-H and dehydrogenation, but the Pt-catalyzed reaction has a lower activation barrier, and the Os-catalyzed reaction is more exothermic. However, differences between functionals once again create a barrier to conclusively predicting whether Pt would favor β-H or o-H dehydrogenation. According to the B3PW91 results, the barrier to β-H dehydrogenation is lower, but according to PBEPBE results, the barrier to *o*-H dehydrogenation is lower. For both functionals, the Pt-catalyzed β-H dehydrogenation reaction is much more exothermic than the Pt-catalyzed *o*-H dehydrogenation reaction.

3.2.4 Energies of dehydrogenation by the same group of metals

a.

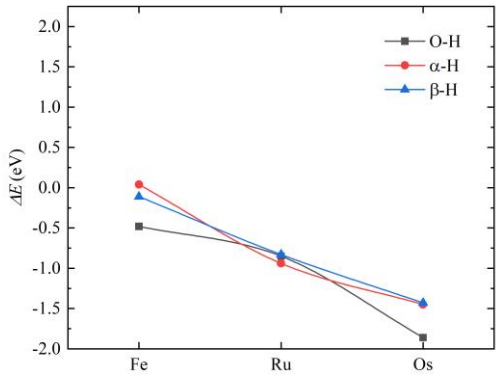

b.

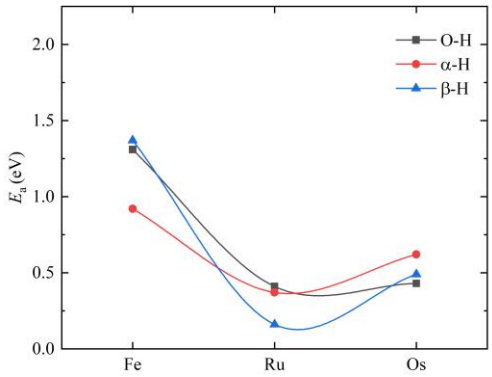

c.

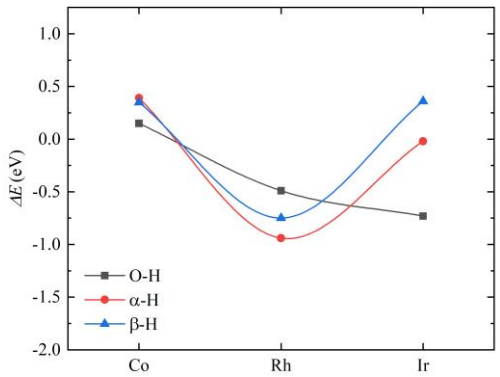

d.

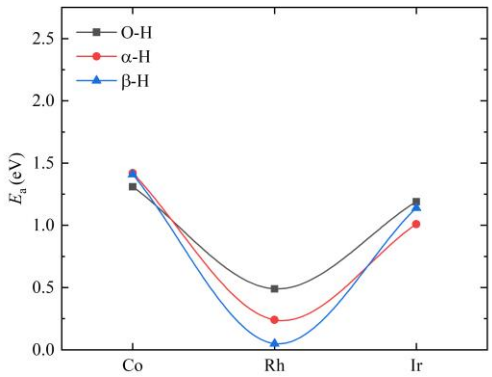

e.

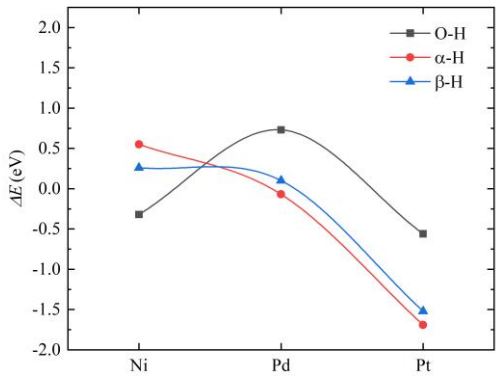

f.

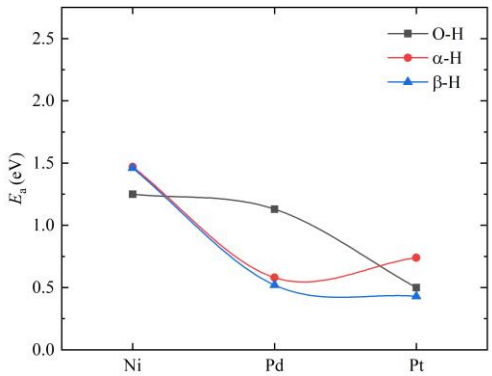

g. h.

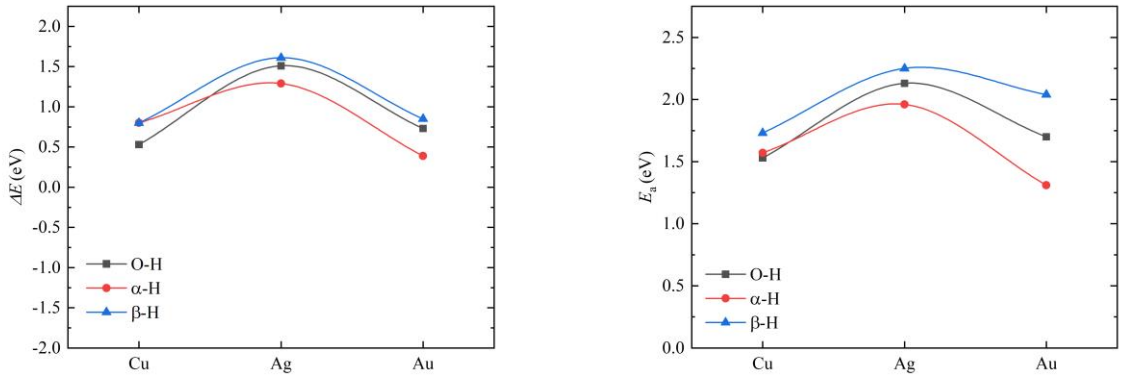

Figure 6: Reaction energies and activation energies calculated using the B3PW91 functional, of a,b) group 8 metals, c,d) group 9 metals, e,f) group 10 metals, and g,h) group 11 metals.

In Figure 6, the reaction energies and activation energies of ethanol dehydrogenation are displayed in an alternative way, in order to see the trend in energy for each group of metals on the periodic table that were investigated. In terms of reaction energies, for group 8, those of α-H and β-H cleavage are similar for the first two metals, with Ru being slightly larger than Fe, then decrease for Os. On the other hand, reaction energy of *o*-H decreases from Fe to Ru. Activation barrier for all three types of dehydrogenation paths of Fe are relatively higher than Ru and Os. For group 9 metals, only the *o*-H cleavage reaction becomes more thermodynamically favorable moving down the group. The α-H and β-H cleavage reactions are much more favorably catalyzed by the 4d metal, Rh. Based on the data in Fig. 6d, it appears the activation energy follows a similar trend to reaction energy for the α-H and β-H, with Rh having the lowest energy. In the case of Ir, α-H is the most feasible reaction on a single Ir, but it is the β-H cleavage the easiest on Ir(100).[105] The selectivity in dehydrogenate different hydrogen atoms may also be tuned using cluster size of the catalysts,[106-121] which ranging from single atom to bulk surfaces.

The reaction energies of the group 10 metals decrease down the group for the α-H and β-H cleavage of ethanol, with a significant decrease in these reaction energies from the 4d to 5d metal. However, this same trend is not observed for the *o*-H bond cleavage by group 10 metals. For these metals, the reaction energy of the 4d metal, Pd, for *o*-H bond cleavage is much higher than for the other two metals in the group. Looking at the activation energy of the dehydrogenation reactions for the group 10 metals, they primarily decrease down the group, besides the rise in energy of Pt-catalyzed α-H dehydrogenation.

Lastly, it appears that for the group 11 metals, the dehydrogenation reactions are more favorably catalyzed by the 3d and 5d metal than by the 4d metal, both thermodynamically and kinetically. The increase in the energy of the 4d metal-catalyzed reactions is more significant for the reaction energy, but also appears for the kinetic energy.

a.

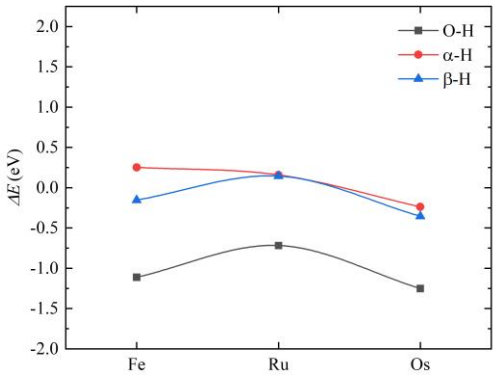

b.

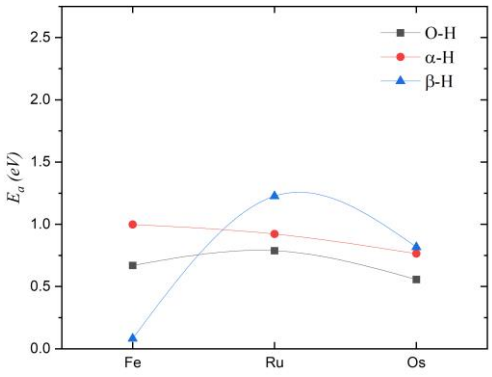

c.

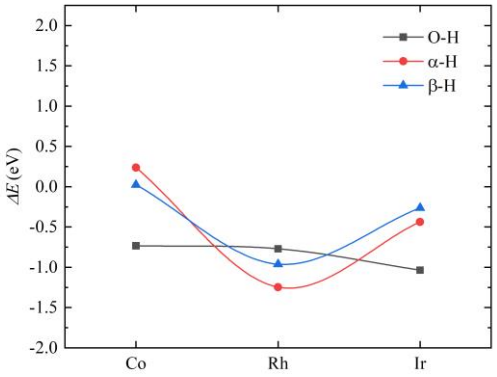

d.

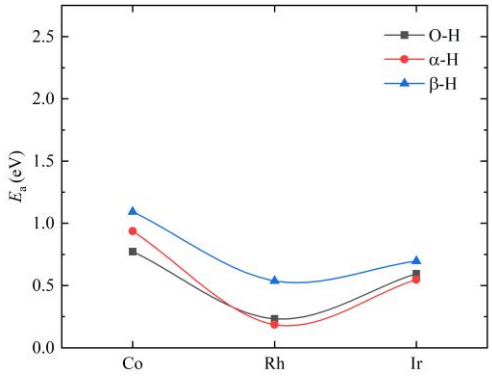

e.

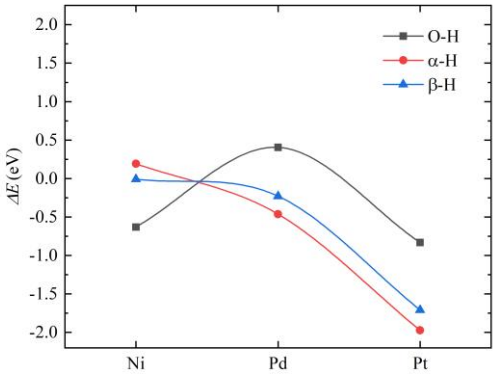

f.

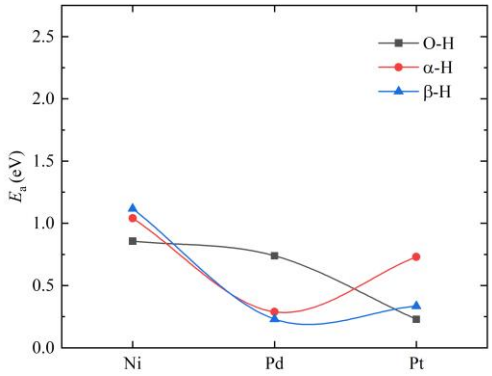

g. h.

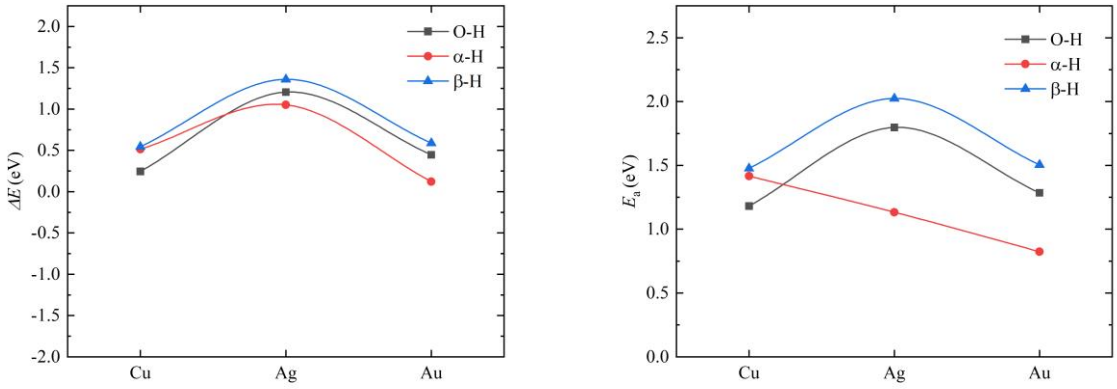

Figure 7: Reaction energies and activation energies calculated using the PBEPBE functional, of a,b) group 8 metals, c,d) group 9 metals, e,f) group 10 metals, and g,h) group 11 metals.

Just as reaction energy and activation energy were plotted in Figure 6 for groups 8, 9, 10, and 11 using B3PW91 results, this was also done for PBEPBE results in Figure 7. In comparison between the B3PW91 and PBEPBE plots, there is a visual similarity between most of the figures, though none exactly the same. Overall, it seems that for each group, there is greater resemblance between the trends in energy for α-H and β-H dehydrogenation than for *o*-H dehydrogenation. It also appears that for groups 9, 10, and 11, the first metal in the group, the 3d metal, prefers *o*-H cleavage, whereas the 4d and 5d metals mainly prefer α-H and β-H cleavage. This "preference" is based on the reaction having both a negative reaction energy, or smallest as in the case of group 11 metals, and the lowest activation barrier.

3.3 Best catalysts for ethanol dehydrogenation

Despite the differences in some results depending on the functional used, some likely catalysts for each type of dehydrogenation can be predicted. Out of all of the metals studied, Sc seems to be the best catalyst for *o*-H dehydrogenation of ethanol, since this reaction has the lowest activation barrier and most exothermic reaction energy with the adsorption of a Sc atom. As for β-H dehydrogenation, this reaction has the lowest energy barrier when catalyzed by Pt. Due to the differences in results between the two functionals, it is difficult to determine whether Pt would prefer to catalyze β-H or *o*-H dehydrogenation. Lastly, it is predicted that the best catalyst for α-H cleavage would be also Pt. Rh is another interesting atom that has lower dehydrogenation activity. To illustrate further the details of the activation of dehydrogenation by Sc, Pt, and Rh, we plotted the structures and energetics of the catalytic steps in Figures 8-10.

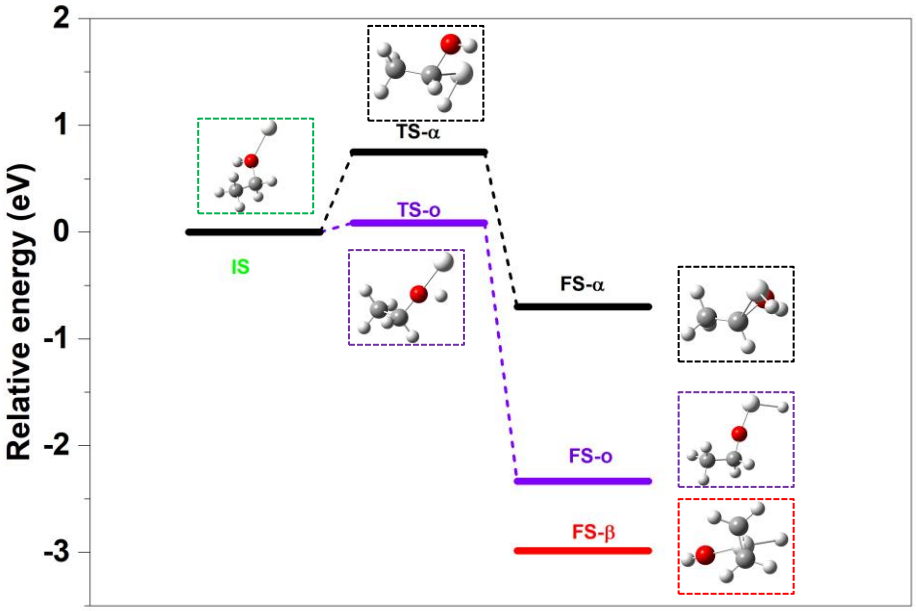

Figure 8: Energies and structures of dehydrogenation in the presence of a Sc atom obtained using the PBEPBE. The gray, red, small white, and bigger white balls correspond to the C, O, H, and Sc atom, respectively.

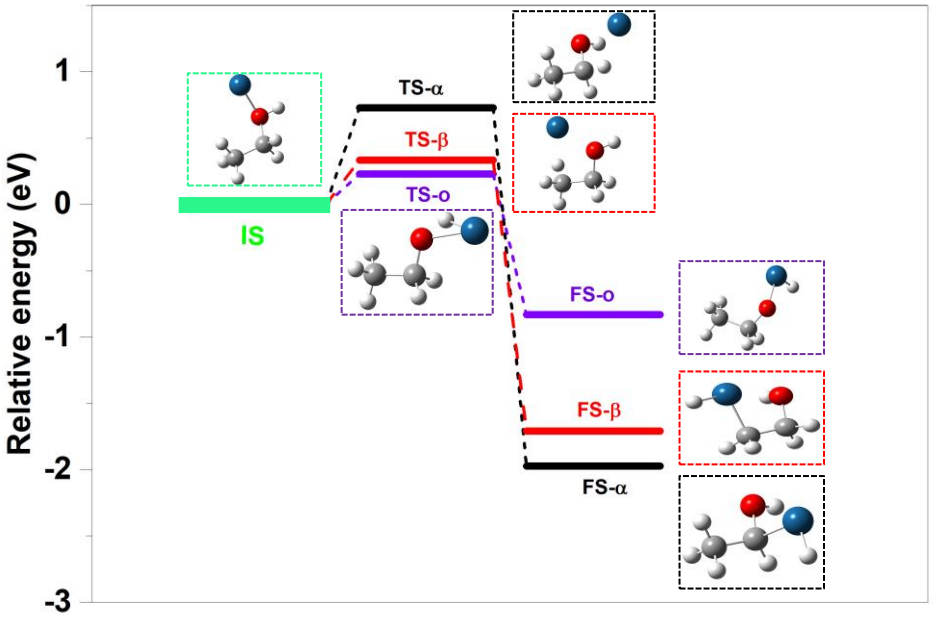

Figure 9: Energies and structures of dehydrogenation in the presence of a Sc atom obtained using the PBEPBE. The gray, red, white, and blue balls correspond to the C, O, H, and Pt atom, respectively.

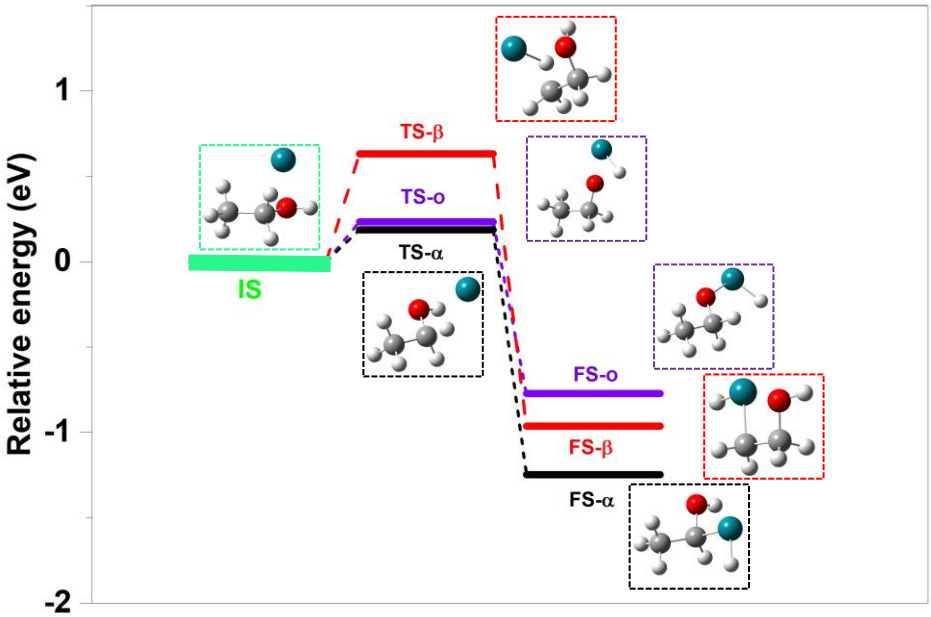

Figure 10: Energies and structures of dehydrogenation in the presence of a Sc atom obtained using the PBEPBE. The gray, red, white, and blue balls correspond to the C, O, H, and Rh atom, respectively.

Finally, we note that it is encouraging that Sc, a 3d metal, appears to be a favorable catalyst for the *o*-H dehydrogenation of ethanol based on both B3PW91 and PBEPBE calculations. While Sc is not the cheapest or most abundant of the 3d metals, it is certainly more so than most of the 4d and 5d metals shown in Figures 3 and 4. These results could be a significant piece of data in the search for an environmentally and economically suitable catalyst for ethanol dehydrogenation.

4. Conclusions

In this work, removal of the α-H, β-H, and *o*-H of ethanol using single atom metals as catalysts was studied using DFT calculations. Gaussian16 was used to perform calculations using two

different functionals, B3PW91 and PBEPBE, in order to evaluate any variation between the two. In most cases, the reaction and activation energies computed using the PBEPBE functional were smaller or more negative than those computed using the B3PW91 functional. This difference, in some cases, was significant enough to lead to inconsistent conclusions about the catalytic ability of a metal in an ethanol dehydrogenation reaction. For most of the reactions, the reaction energies calculated using the PBEPBE functional were around 0.1-0.4 eV lower than those calculated using the B3PW91 functional. Still, the results of both functionals were analyzed to predict the best catalysts for each ethanol dehydrogenation reaction. Pt was found to be the best catalysts for both α-H and β-H ethanol dehydrogenation reaction. Sc was found for the *o*-H ethanol dehydrogenation. There is some uncertainty in whether Pt would prefer α-H or β-H dehydrogenation reaction first.

ACKNOWLEDMENTS

KRW acknowledges the support through the REACH program at SIUC. DC acknowledges the support by the National Science Foundation (REU-DMR-1757954).

REFERENCES

(1) Huang, Y.; Wang, B.; Yuan, H.; Sun, Y.; Yang, D.; Cui, X.; Shi, F. *Catal. Sci. Technol.* **2021**, *11*, 1652.
(2) IEA(2020) Paris, 2020; Vol. 2023.
(3) CAPP; Vol. 2023.
(4) Biofuels explained 2020; Vol. 2021.
(5) Bioenergy Technologies Office; Bioenergy Technologies Office; Vol. 2023.
(6) Ogo, S.; Sekine, Y. *Fuel Process. Technol.* **2020**, *199*, 106238.
(7) Sun, H.; Liu, D.; Wang, T.; Lu, T.; Li, W.; Ren, S.; Hu, W.; Wang, L.; Zhou, X. *ACS Appl. Mater. Interfaces* **2017**, *9*, 9880.
(8) Xu, F.; Testoff, T. T.; Wang, L.; Zhou, X. *Molecules* **2020**, *25*, 4478.
(9) Liang, Y.; Liu, M.; Wang, T.; Mao, J.; Wang, L.; Liu, D.; Wang, T.; Hu, W. *Adv. Mater.* **2023**, 2304820.
(10) Wang, T.; Zhao, C.; Zhang, L.; Lu, T.; Sun, H.; Bridgmohan, C. N.; Weerasinghe, K. C.; Liu, D.; Hu, W.; Li, W.; Zhou, X.; Wang, L. *J. Phys. Chem. C* **2016**, *120*, 25263.
(11) Wang, W.; Lv, F.; Lei, B.; Wan, S.; Luo, M. C.; Guo, S. J. *Adv. Mater.* **2016**, *28*, 10117.
(12) Wang, T.; Weerasinghe, K. C.; Ubaldo, P. C.; Liu, D.; Li, W.; Zhou, X.; Wang, L. *Chem. Phys. Lett.* **2015**, *618*, 142.
(13) Zhou, X.; Liu, D.; Wang, T.; Hu, X.; Guo, J.; Weerasinghe, K. C.; Wang, L.; Li, W. *J. Photochem. Photobiol. A: Chem.* **2014**, *274*, 57.

(14) Walkup, L. L.; Weerasinghe, K. C.; Tao, M.; Zhou, X.; Zhang, M.; Liu, D.; Wang, L. *J. Phys. Chem. C* **2010**, *114*, 19521.
(15) McCarroll, M. E.; Shi, Y.; Harris, S.; Puli, S.; Kimaru, I.; Xu, R.; Wang, L.; Dyer, D. J. *J. Phys. Chem. B* **2006**, *110*, 22991.
(16) Zheng, Y.; Chen, Y.; Cao, Y.; Huang, F.; Guo, Y.; Zhu, X. *ACS Mater. Lett.* **2022**, *4*, 882.
(17) Zeng, L.; Huang, L.; Han, J.; Han, G. *Acc. Chem. Res.* **2022**, *55*, 2604.
(18) Xu, C.; Zhao, Z.; Yang, K.; Niu, L.; Ma, X.; Zhou, Z.; Zhang, X.; Zhang, F. *J. Mater. Chem. A* **2022**, *10*, 6291.
(19) Venkatesan, S.; Hsua, T.-H.; Wong, X.-W.; Teng, H.; Lee, Y.-L. *Chem. Eng. J.* **2022**, *446*, 137349.
(20) Sharif, O. F. A.; Nhari, L. M.; El-Shishtawy, R. M.; Zayeda, M. E. M.; Asiri, A. M. *RSC Adv.* **2022**, *12*, 19270.
(21) Nagaraju, N.; Kushavah, D.; Kumar, S.; Ray, R.; Gambhir, D.; Ghosh, S.; Pal, S. K. *Phys. Chem. Chem. Phys.* **2022**, *24*, 3303.
(22) Li, J.; Dong, Y.; Wei, R.; Jiang, G.; Yao, C.; Lv, M.; Wu, Y.; Gardner, S. H.; Zhang, F.; Lucero, M. Y.; Huang, J.; Chen, H.; Ge, G.; Chan, J.; Chen, J.; Sun, H.; Luo, X.; Qian, X.; Yang, Y. *J. Am. Chem. Soc.* **2022**, *144*, 14351.
(23) Geng, Y.; Zhang, G.; Chen, Y.; Peng, Y.; Wang, X.; Wang, Z. *Anal. Chem.* **2022**, *94*, 1813.
(24) Feng, Q.; Yang, T.; Ma, L.; Li, X.; Yuan, H.; Zhang, M.; Zhang, Y.; Fan, L. *ACS Appl. Mater. Interfaces* **2022**, *14*, 38594.
(25) Zhang, Z.; Ho, J. K. W.; Zhang, C.; Yin, H.; Wen, Z.; Cai, G.; Zhao, R.; Shi, R.; Lu, X.; Liu, J.; Hao, X.; Cheng, C.; So, S. K. *J. Mater. Chem. C* **2021**, *9*, 12281.
(26) Crivello, M.; Pérez, C.; Fernández, J.; Eimer, G.; Herrero, E.; Casuscelli, S.; Rodríguez-Castellón, E. *Appl. Catal. A Gen.* **2007**, *317*, 11.
(27) Sun, J.; Wang, Y. *ACS Catal.* **2014**, *4*, 1078.
(28) Eagan, N. M.; Kumbhalkar, M. D.; Buchanan, J. S.; Dumesic, J. A.; Huber, G. W. *Nat. Rev. Chem.* **2019**, *3*, 223.
(29) Burhan, H. Y., M.; Cellat, K.; Zeytun, A.; Yilmaz, G.; Sen, F. *Direct Liquid Fuel Cells* **2021**, 95.
(30) Wu, R.; Wang, L. *J. Phys. Chem. C* **2020**, *124*, 26953.
(31) Wu, R.; Wang, L. *J. Phys. Chem. C* **2022**, *126*, 21650.
(32) Wu, R.; Wang, L. *Phys. Chem. Chem. Phys.* **2023**, *25*, 2190.
(33) Badwal, S. P. S.; Giddey, S.; Kulkarni, A.; Goel, J.; Basu, S. *Appl. Energy* **2015**, *145*, 80.
(34) Wu, C.; Wang, L.; Xiao, Z.; Li, G.; Wang, L. *Chem. Phys. Lett.* **2020**, *746*, 137229.
(35) Wu, R.; Wiegand, K. R.; Ge, L.; Wang, L. *J. Phys. Chem. C* **2021**, *125*, 14275.
(36) Wu, C.; Wang, L.; Xiao, Z.; Li, G.; Wang, L. *Phys. Chem. Chem. Phys.* **2020**, *22*, 724.
(37) Yaqoob, L.; Noor, T.; Iqbal, N. *RSC Adv.* **2021**, *11*, 16768.
(38) Wu, R.; Wang, L. *ChemPhysChem* **2022**, *23*, e202200132.
(39) Wala, M.; Simka, W. *Molecules* **2021**, *26*, 2144.
(40) Luo, S.; Zhang, L.; Liao, Y.; Li, L.; Yang, Q.; Wu, X.; Wu, X.; He, D.; He, C.; Chen, W.; Wu, Q.; Li, M.; Hensen, E. J. M.; Quan, Z. *Adv. Mater.* **2021**, *33*, 2008508.
(41) Altarawneh, R. M. *Energy Fuels* **2021**, *35*, 11594.
(42) Zhao, X.; Liu, Q.; Li, Q.; Chena, L.; Mao, L.; Wang, H.; Chen, S. *Chem. Eng. J.* **2020**, *400*, 125744.
(43) Yang, X.; Liang, Z.; Chen, S.; Ma, M.; Wang, Q.; Tong, X.; Zhang, Q.; Ye, J.; Gu, L.; Yang, N. *Small* **2020**, *16*, 2004727.
(44) Lyu, F. L.; Cao, M. H.; Mahsud, A.; Zhang, Q. *J. Mater. Chem. A* **2020**, *8*, 15445.
(45) Bepari, S.; Kuila, D. *Int. J. Hydrog. Energy* **2020**, *45*, 18090.
(46) Zhu, C.; Lan, B.; Wei, R.-L.; Wang, C.-N.; Yang, Y.-Y. *ACS Catal.* **2019**, *9*, 4046.

(47) Miao, B.; Wu, Z.-P.; Xu, H.; Zhang, M.; Chen, Y.; Wang, L. *Comput. Mater. Sci.* **2019**, *156*, 175.
(48) Taghizadeh, M.; Aghili, F. *Rev. Chem. Eng.* **2019**, *35*, 377.
(49) Rizo, R.; Perez-Rodriguez, S.; Garcia, G. *ChemElectroChem* **2019**, *6*, 4725.
(50) Peera, S. G.; Lee, T. G.; Sahu, A. K. *Sustain. Energy Fuels* **2019**, *3*, 1866.
(51) Marinkovic, N. S.; Li, M.; Adzic, R. R. *Topics Current Chem.* **2019**, *377*, 11.
(52) Hui, Y. H.; Zhang, S. W.; Wang, W. T. *Adv. Syn. Catal.* **2019**, *361*, 2215.
(53) Chang, Q.; Kattel, S.; Li, X.; Liang, Z.; Tackett, B. M.; Denny, S. R.; Zhang, P.; Su, D.; Chen, J. G.; Chen, Z. *ACS Catal.* **2019**, *9*, 7618.
(54) Bai, J.; Liu, D. Y.; Yang, J.; Chen, Y. *ChemSusChem* **2019**, *12*, 2117.
(55) Zhang, J.; Ye, J.; Fan, Q.; Jiang, Y.; Zhu, Y.; Li, H.; Cao, Z.; Kuang, Q.; Cheng, J.; Zheng, J.; Xie, Z. *J. Am. Chem. Soc.* **2018**, *140*, 11232.
(56) Zaccheria, F.; Scotti, N.; Ravasio, N. *Chemcatchem* **2018**, *10*, 1526.
(57) Liu, Y.; Wei, M.; Raciti, D.; Wang, Y.; Hu, P.; Park, J. H.; Barclay, M.; Wang, C. *ACS Catal.* **2018**, *8*, 10931.
(58) Sharma, Y. C.; Kumar, A.; Prasad, R.; Upadhyay, S. N. *Renew. Sustain. Energy Rev.* **2017**, *74*, 89.
(59) Xu, H.; Miao, B.; Zhang, M.; Chen, Y.; Wang, L. *Phys. Chem. Chem. Phys.* **2017**, *19*, 26210.
(60) Wu, Z.; Zhang, M.; Jiang, H.; Zhong, C.-J.; Chen, Y.; Wang, L. *Phys. Chem. Chem. Phys.* **2017**, *19*, 15444.
(61) Miao, B.; Wu, Z.; Xu, H.; Zhang, M.; Chen, Y.; Wang, L. *Chem. Phys. Lett.* **2017**, *688*, 92.
(62) Wu, R. W., K. R.; Wang, L. *J. Chem. Phys.* **2021**, *154*, 054705.
(63) Sun, K.; Zhang, M.; Wang, L. *Chem. Phys. Lett.* **2013**, *585*, 89.
(64) Wu, R.; Sun, K.; Chen, Y.; Zhang, M.; Wang, L. *Surf. Sci.* **2021**, *703*, 121742.
(65) Wu, R.; Wang, L. *Chem. Phys. Lett.* **2017**, *678*, 196.
(66) Wu, R.; Wang, L. *Comput. Mater. Sci.* **2021**, *196*, 110514.
(67) Rioux, R.; Vannice, M. *J. Catal.* **2005**, *233*, 147.
(68) Guan, Y.; Hensen, E. J. M. *Appl. Catal. A Gen.* **2009**, *361*, 49.
(69) Sushkevich, V. L.; Ivanova, I. I.; Taarning, E. *ChemCatChem* **2013**, *5*, 2367.
(70) Giannakakis, G.; Kress, P.; Duanmu, K.; Ngan, H. T.; Yan, G.; Hoffman, A. S.; Qi, Z.; Trimpalis, A.; Annamalai, L.; Ouyang, M.; Liu, J.; Eagan, N.; Biener, J.; Sokaras, D.; Flytzani-Stephanopoulos, M.; Bare, S. R.; Sautet, P.; Sykes, E. C. H. *J. Am. Chem. Soc.* **2021**, *143*, 21567.
(71) Hou, C.; Li, Y.; Ke, Z. *Inorg. Chim. Acta* **2020**, *511*, 119808.
(72) Xiao, F.; Wang, Q.; Xu, G.-L.; Qin, X.; Hwang, I.; Sun, C.-J.; Liu, M.; Hua, W.; Wu, H.-W.; Zhu, S.; Li, J.-C.; Wang, J.-G.; Zhu, Y.; Wu, D.; Wei, Z.; Gu, M.; Amine, K.; Shao, M. *Nat. Catal.* **2022**, *5*, 503.
(73) Shen, T.; Wang, S.; Zhao, T.; Hu, Y.; Wang, D. *Adv. Energy Mater.* **2022**, *12*, 2201823.
(74) Shah, S. S. A.; Najam, T.; Bashir, M. S.; Javed, M. S.; Rahman, A.-u.; Luque, R.; Bao, S.-J. *Small* **2022**, *18*, 2106279
(75) Xiao, F.; Liu, X.; Sun, C.-J.; Hwang, I.; Wang, Q.; Xu, Z.; Wang, Y.; Zhu, S.; Wu, H.-W.; Wei, Z.; Zheng, L.; Cheng, D.; Gu, M.; Xu, G.-L.; Amine, K.; Shao, M. *Nano Lett.* **2021**, *21*, 3633.
(76) Zhao, D.; Zhuang, Z. W.; Cao, X.; Zhang, C.; Peng, Q.; Chen, C.; Li, Y. D. *Chem. Soc. Rev.* **2020**, *49*, 2215.
(77) Zhu, C. Z.; Fu, S. F.; Shi, Q. R.; Du, D.; Lin, Y. H. *Angew. Chem. Int. Ed.* **2017**, *56*, 13944.
(78) Wang, C. Y.; Yang, M.; Flytzani-Stephanopoulos, M. *Aiche Journal* **2016**, *62*, 429.
(79) Wang, Y.; Su, H.; He, Y.; Li, L.; Zhu, S.; Shen, H.; Xie, P.; Fu, X.; Zhou, G.; Feng, C.; Zhao, D.; Xiao, F.; Zhu, X.; Zeng, Y.; Shao, M.; Chen, S.; Wu, G.; Zeng, J.; Wang, C. *Chem. Rev.* **2020**, *120*, 12217.
(80) Hoa, V. H.; Prabhakaran, S.; Lea, K. T. N.; Kim, D. H. *J. Mater. Chem. A* **2022**, *10*, 14604.

(81) Singh, B.; Gawande, M. B.; Kute, A. D.; Varma, R. S.; Fornasiero, P.; McNeice, P.; Jagadeesh, R. V.; Beller, M.; Zbořil, R. *Chem. Rev.* **2021**, *121*, 13620.
(82) Hannagan, R. T.; Giannakakis, G.; Réocreux, R.; Schumann, J.; Finzel, J.; Wang, Y.; Michaelides, A.; Deshlahra, P.; Christopher, P.; Flytzani-Stephanopoulos, M.; Stamatakis, M.; Sykes, E. C. H. *Science* **2021**, *372*, 1444.
(83) Lu, B.; Liu, Q.; Chen, S. *ACS Catal.* **2020**, *10*, 7584.
(84) Chen, Y.; Gao, R.; Ji, S.; Li, H.; Tang, K.; Jiang, P.; Hu, H.; Zhang, Z.; Hao, H.; Qu, Q.; Liang, X.; Chen, W.; Dong, J.; Wang, D.; Li, Y. *Angew. Chem. Int. Ed.* **2021**, *60*, 3212.
(85) Shan, J.; Ye, C.; Jiang, Y.; Jaroniec, M.; Zheng, Y.; Qiao, S.-Z. *Sci. Adv.* **2022**, *8*, eabo0762.
(86) Liu, L.; Li, M.; Chen, F.; Huang, H. *Small Struct.* **2023**, *4*, 2200188.
(87) Denisov, N.; Qin, S.; Will, J.; Vasiljevic, B. N.; Skorodumova, N. V.; Pašti, I. A.; Sarma, B. B.; Osuagwu, B.; Yokosawa, T.; Voss, J.; Wirth, J.; Spiecker, E.; Schmuki, P. *Adv. Mater.* **2023**, *35*, 2206569.
(88) Zhang, Q.; Zheng, L.; Gu, F.; Wu, J.; Gao, J.; Zhang, Y.-C.; Zhu, X.-D. *Nano Energy* **2023**, *116*, 108789.
(89) Allangawi, A.; Gilani, M. A.; Ayub, K.; Mahmood, T. *Int. J. Hydrogen Energy* **2023**, *48*, 16663.
(90) Yan, C.; Liu, Y.-L.; Zeng, Q.; Wang, G.-G.; Han, J.-C. *Adv. Funct. Mater.* **2023**, *33*, 2210837.
(91) Wang, K.; Liu, S.; Shu, Z.; Zheng, Q.; Zheng, M.; Dong, Q. *Phys. Chem. Chem. Phy.* **2023**, *25*, 25942.
(92) Zhu, Y.; Wang, J.; Ma, J. *Small Sci.* **2023**, *3*, 2300010.
(93) Yang, X.-F.; Wang, A.; Qiao, B.; Li, J.; Liu, J.; Zhang, T. *Acct. Chem. Res.* **2013**, *46*, 1740.
(94) Li, H.; Xiong, C.; Fei, M.; Ma, L.; Zhang, H.; Yan, X.; Tieu, P.; Yuan, Y.; Zhang, Y.; Nyakuchena, J.; Huang, J.; Pan, X.; Waegele, M. M.; Jiang, D.-e.; Wang, D. *J. Am. Chem. Soc.* **2023**, *145*, 11415−11419.
(95) Zhang, L. R., Y.; Liu, W.; Wang, A.; Zhang, T *Natl. Sci. Rev.* **2018**, *5*, 653.
(96) Ma, D. W.; Wang, Q.; Yan, X.; Zhang, X.; He, C.; Zhou, D.; Tang, Y.; Lu, Z.; Yang, Z. *Carbon* **2016**, *105*, 463.
(97) Pieta, I. S.; Kadam, R. G.; Pieta, P.; Mrdenovic, D.; Nowakowski, R.; Bakandritsos, A.; Tomanec, O.; Petr, M.; Otyepka, M.; Kostecki, R.; Khan, M. A. M.; Zboril, R.; Gawande, M. B. *Adv. Mater. Interfaces* **2021**, *8*, 2001822.
(98) Vogiatzis, K. D. P., M. V.; Kirkland, J. K.; Hashemi, A.; Liu, C.; Pidko, E. A *Chem. Rev.* **2019**, 2453.
(99) Wang, J. L., C. S.; Lin, M. C *J. Phys. Chem. C* **2009**, *113*, 6681.
(100) Liang, S. H., C.; Shi, Y *ChemCatChem* **2015**, *7*, 2559.
(101) Fajin, J. L.; Vines, F.; MN, D. S. C.; Illas, F.; Gomes, J. R. *J. Chem. Theory. Comput.* **2016**, *12*, 2121.
(102) Zhang, J.; Hu, H.; Liu, X.; Li, D. S. *Materials Today Chemistry* **2019**, *11*, 42.
(103) Yuan, B.; Zhuang, J.; Kirmess, K. M.; Bridgmohan, C. N.; Whalley, A. C.; Wang, L.; Plunkett, K. N. *J. Org. Chem.* **2016**, *81*, 8312.
(104) Bheemireddy, S. R.; Ubaldo, P. C.; Finke, A. D.; Wang, L.; Plunkett, K. N. *J. Mater. Chem. C* **2016**, *4*, 3963.
(105) Wu, R.; Wang, L. *Chem. Phys. Impact* **2021**, *3*, 100040.
(106) Sun, K.; Wu, Z.; Wu, R.; Chen, Y.; Zhang, M.; Wang, L. *ChemRxiv* **2023**, 10.26434/chemrxiv.
(107) Wang, L.; Williams, J. I.; Lin, T.; Zhong, C. J. *Catal. Today* **2011**, *165*, 150.
(108) Lu, J.; Aydin, C.; Browning, N. D.; Wang, L.; Gates, B. C. *Catal. Lett.* **2012**, *142*, 1445.
(109) Wu, C.; Xiao, Z.; Wang, L.; Li, G.; Zhang, X.; Wang, L. *Catal. Sci. Technol.* **2021**, *11*, 1965.
(110) Wang, L.; Ore, R. M.; Jayamaha, P. K.; Wu, Z.-P.; Zhong, C.-J. *Faraday Discuss.* **2023**, *242*, 429.

(111) Jung, J. Y.; Kim, D.-g.; Jang, I.; Kim, N. D.; Yoo, S. J.; Kim, P. *J. Ind. Eng. Chem.* **2022**, *111*, 300.
(112) Gebre, S. H.; Sendeku, M. G. *J. Energy Chem.* **2022**, *65*, 329.
(113) Belenov, S.; Alekseenko, A.; Pavlets, A.; Nevelskaya, A.; Danilenko, M. *Catalysts* **2022**, *12*, 638.
(114) Matsuda, S.; Masuda, S.; Takano, S.; Ichikuni, N.; Tsukuda, T. *ACS Catal.* **2021**, *11*, 10502.
(115) Huang, L.; Zaman, S.; Wang, Z. T.; Niu, H. T.; You, B.; Xia, B. Y. *Acta Physico-Chimica Sinica* **2021**, *37*, 2009035.
(116) Han, S. M.; He, C. H.; Yun, Q. B.; Li, M. Y.; Chen, W.; Cao, W. B.; Lu, Q. P. *Coord. Chem. Rev.* **2021**, *445*, 214085.
(117) Bueno, S. L. A.; Ashberry, H. M.; Shafei, I.; Skrabalak, S. E. *Acc. Chem. Res.* **2021**, *54*, 1662.
(118) Yang, T. Y.; Cui, C.; Rong, H. P.; Zhang, J. T.; Wang, D. S. *Acta Physico-Chimica Sinica* **2020**, *36*, 2003047.
(119) Chen, C. Y.; Song, T. X.; Shang, H. Y.; Liu, Q. Y.; Yuan, M. Y.; Wang, C.; Du, Y. K. *Int. J. Hydrogen Energy* **2020**, *45*, 26920.
(120) Axet, M. R.; Philippot, K. *Chem. Rev.* **2020**, *120*, 1085.
(121) Xia, Y.; Yang, H.; Campbell, C. T. *Acct. Chem. Res.* **2013**, *46*, 1671.